HHS Public Access

Author manuscript

*Int J Pharm*. Author manuscript; available in PMC 2016 February 20.

Published in final edited form as:

*Int J Pharm*. 2015 February 20; 479(2): 329–337. doi:10.1016/j.ijpharm.2014.12.052.

# Preparation and *In Vitro* Evaluation of Hydrophilic Fenretinide Nanoparticles

**Grace A. Ledet**, **Richard A. Graves**, **Elena Y. Glotser**, **Tarun K. Mandal**, and **Levon A. Bostanian***

College of Pharmacy, Division of Basic Pharmaceutical Sciences, Xavier University of Louisiana, 1 Drexel Drive, New Orleans, LA 70125

## Abstract

Fenretinide is an effective anti-cancer drug with high *in vitro* cytotoxicity and low *in vivo* systemic toxicity. In clinical trials, fenretinide has shown poor therapeutic efficacy following oral administration – attributed to its low bioavailability and solubility. The long term goal of this project is to develop a formulation for the oral delivery of fenretinide. The purpose of this part of the study wasto prepare and characterize hydrophilic nanoparticle formulations of fenretinide. Three different ratios of polyvinyl pyrrolidone (PVP) to fenretinide were used, namely, 3:1, 4:1, and 5:1. Both drug and polymer were dissolved in a mixture of methanol and dichloromethane (2:23 v/v). Rotary evaporation was used to remove the solvents, and, following reconstitution with water, a high pressure homogenizer was used to form nanoparticles. The particle size and polydispersity index were measured before and after lyophilization. The formulations were studied by scanning electron microscopy (SEM), differential scanning calorimetry (DSC), and x-ray powder diffraction (XRPD). The effectiveness of the formulations was assessed by releasestudies and Caco-2 cell permeability assays. As the PVP content increased, the recovered particle size following lyophilization became more consistent with the pre-lyophilization particle size, especially for those formulations with less lactose. The DSC scans of the formulations did not show any fenretinide melting endotherms, indicating that the drug was either present in an amorphous form in the formulation or that a solid solution of the drug in PVP had formed. For the release studies, the highest drug release among the formulations was 249.2 ± 35.5 ng/mL for the formulation with 4:1 polymer-to-drug. When the permeability of the formulations was evaluated in a Caco-2 cell model, the mean normalized flux for each treatment group was significantly higher ($p<0.05$) from the fenretinide control. The formulation containing 4:1 polymer-to-drug ratio and 6:5 lactose-to-formulation ratio emerged as the optimal choice for further evaluation as a potential oral delivery formulation for fenretinide.



*Corresponding Author Levon A. Bostanian, Ph.D. College of Pharmacy Xavier University of Louisiana 1 Drexel Dr. New Orleans, LA 70125-1098 Phone: (504) 520-7423 Fax: (504) 520-7954 lbostani@xula.edu.

**Keywords**

Fenretinide; formulation; PVP; nanoparticles; permeability

## Introduction

The synthetic retinoid fenretinide, N-4-hydroxyphenyl retinamide or 4-HPR, was first synthesized in the late 1960's and first investigated for prevention of breast cancer in rats in 1979 due to its selective accumulation in breast tissue [1]. While the mechanism of action is not fully elucidated, fenretinide does inhibit cell growth through apoptosis rather than just differentiation, distinguishing fenretinide from other retinoic acid derivatives [2,3]. Since the initial investigations in mammary carcinoma, fenretinide research has expanded to include breast cancer chemoprevention [4,5] and the treatment of age-related macular degeneration [6] – yet the largest thrust of research is still in cancer treatment. Fenretinide has demonstrated cytotoxicity in many cancer cell lines, and in over 35 cancer clinical trials, fenretinide has been studied in cancers such as breast [7], prostate [8], kidney [9], ovarian [10], oral leukoplakia [11], bladder [12], small cell lung cancer [13], and neuroblastoma [14] – generally producing disappointing, marginal results.

Fenretinide's poor therapeutic efficacy in clinical trials, despite ample evidence of its low toxicity *in vivo* and its cytotoxic effects *in vitro*, is often attributed to its low bioavailability following oral delivery in a capsule [9,11,14,15]. Fenretinide is usually administered in a gelatin capsule with corn oil and polysorbate 80. Clinical trial patients are oftenrequired to takemany capsules to reach the required dosage level and report having difficulty swallowing the capsules [7]. Similarly, in clinical trials with children, patients received 5 to 14 capsules per dose, making administration challenging and inconsistent [14]. High doses of fenretinide, in studies where dose escalation was not precluded by the number of capsules required, did not translate into higher serum levels [8,9,11,16].

The clear direction of fenretinide's future as a chemotherapeutic agent is to improve its dosage form and bioavailability. LYM-X-SORB is a lipid matrix composed of lysophosphatidylcholine, monoglyceride, and free fatty acids [17], and this oral formulation of fenretinide was made to overcome the patient compliance and bioavailability issues observed with the corn oil capsule dosage form. However, when evaluated in adults, the mean plasma levels of fenretinide using the LYM-X-SORB formulation were no better than the corn oil capsules, and GI complaints caused 7 out of the 20 patients to withdraw from the study [18].

The bioavailability of a drug following oral delivery can be hindered by many factors such as poor aqueous solubility, first-pass metabolism, and/or poor or incomplete absorption in the gastrointestinal tract. Solid dispersions of drugs aim to improve the bioavailability of poorly water soluble drugs, like fenretinide, by improving their dissolution rates through a reduction in particle size and improvement of drug dissolution [19-21]. Improving the dissolution rate by formulation as a solid dispersion results in a high drug concentration gradient across the gastrointestinal lumen, which may translate into improved blood plasma concentrations following oral delivery [22]. In solid dispersions, the drug form can range

from crystalline to fully amorphous. An amorphous drug state generally results in faster dissolution rates, resulting in better oral bioavailability, but with the caveat that the drug is in a more unstable state [23,24]. Polyvinylpyrrolidone (PVP) is one of the most common polymers used to formulate solid dispersions because of its low toxicity, high aqueous solubility, and good physiological tolerance [25-28]. One way that PVP enhances drug dissolutionis by inhibition of crystallization of the drug by PVP's anti-plasticizing effect[29].

The goal of the present study is to evaluate PVP-based nanoparticles as a means to increase the permeability of fenretinide through the gut. PVP-fenretinide solid dispersions were prepared by solvent evaporation and high pressure homogenization, and characterized by their particle size, morphology, thermal properties, and by drug releasestudies. Caco-2 cell studies were performed to assess the *in vitro* intestinal cellular permeability of the PVP-fenretinide formulations.

## Materials and Methods

### Materials

Fenretinide was purchased from R&D Systems, Inc. (Minneapolis, MN). Polyvinylpyrrolidone (MW 40,000), α-lactose monohydrate, methanol, dichloromethane, ethanol, bovine serum albumin, HEPES, glucose, sodium chloride, potassium chloride, calcium chloride, magnesium chloride, sodium phosphate monobasic, potassium phosphate dibasic, sodium hydroxide, hydrochloric acid, formic acid, Hanks' Balanced Salt Solution (HBSS), and Lucifer yellow were purchased from Sigma-Aldrich (St. Louis, MO). All cell culture media were purchased from Thermo Fisher Scientific (Waltham, MA).

### Preparation of Formulations

Three different ratios of polyvinylpyrrolidone (PVP) to fenretinide were used namely, 3:1, 4:1, and 5:1. Both drug and polymer were dissolved in a mixture of methanol and dichloromethane (2:23 v/v). The solvents were then removed by evaporation using rotary evaporation at 80°C and 100 RPM, and a thin film of fenretinide and PVP was obtained. This thin film was reconstituted with 3.0 mL of water and sonicated with a bath sonicator to ensure complete recovery of the material. The formulations were then homogenized for 20 passes at 16,000 psi using a high pressure homogenizer (EmulsiFlex-B3, Avestin Inc., Ottawa, Ontario, Canada). Lactose was added as a stabilizer at two different amounts (30 mg and 60 mg), the formulations were frozen at −20°C, and finally the formulations were lyophilized at −20°C for 48 hours using a FreeZone 6 Freeze Dry System (Labconco, Kansas City, MO). All formulations were prepared in triplicate. The formulation compositions are presentedin Table 1. In addition, aphysical mixture of PVP, fenretinide, and lactose,with a composition corresponding to formulation A2,was prepared by trituration using a mortar and pestle until a homogeneous mixture was obtained and passed through a #80 mesh sieve (sieve opening size of 180 μm). Drug recovery was measured by UV spectroscopy (DU 640 spectrophotometer, Beckman Coulter, Inc., Fullerton, CA) at 230 nm by dissolving 2 mg of each formulation in methanol.

### Particle Size

The particle size and distribution weremeasured by using a DelsaNano C Particle Analyzer (Beckman Coulter, Inc., Fullerton, CA). This equipment uses photon correlation spectroscopy, which determines the particle size based on the rate of intensity fluctuations of a laser scattered by the particles. Measurements were done before and after lyophilization to determine if the particle size was recovered following reconstitution of the powdered formulations. All samples were reconstituted with double-deionized water immediately prior to size analysis by vortexing for 30 seconds. All measurements were done in triplicate.

### Scanning Electron Microscopy (SEM)

Scanning electron microscopy (SEM) (S-4800, Hitachi High Technologies America Inc., Gaithersburg, MD) was used to observe the formulations and confirm their morphology and size distribution. Powdered samplesof the physical mixture and the formulations were mounted on SEM stubswith carbon tape. Additionally, the formulations were re-dispersed in water, briefly sonicated, and dried on carbon tape under vacuum. All samples were gold sputter-coated at 2.0 mA for 1 minute (K550X Sputter Coater, Quorum Technologies Ltd, West Sussex, UK). An accelerating voltage of 5 kV was used for all SEM observations.

### Differential Scanning Calorimetry

Thermal analysis was carried out by differential scanning calorimetry (DSC) (Q2000, TA Instruments, New Castle, DE). Samples were prepared in sealed aluminum pans. Modulated DSC (MDSC) was employed ramping at 3°C/min from 20°C to 300°C and at a modulation rate of +/− 1°C/60 sec.

### X-ray Powder Diffraction

The samples were analyzed by x-ray powder diffraction (XRPD) (MiniFlex II Desktop X-ray Powder Diffractometer, Rigaku Corporation, Tokyo, Japan) to determine the crystalline state of the drug in the formulations. The powdered formulations and physical mixture were each dispersed in minimal water, deposited onto a glass slide, frozen at −20°C, and lyophilized overnight. Control samples of PVP, lactose, and fenretinide were prepared for comparison. The samples were analyzed over $2\theta$ range of 5° to 50° with a count time of 4 s.

### Release Study

*In vitro*release tests were carried out in simulated intestinal fluid (SIF) without protein (pH = 6.8) using a CP 7*smart* USP Apparatus 4 Flow-Through Cell Dissolution system (SOTAX Corporation, Westborough, MA). Approximately 3 mg of each batch(three batches for each formulation) was used for each test in the 5 mL sample cells, and 500 mL vessels were used in the closed loop configuration. The samples were run at a flow rate of 16 mL/min, at a pump speed of 120 r/min, at 37°C, and with sampling times at 0.25 h, 0.5 h, 1 h, 3 h, 6 h, and 24 h. At each time point, the samples were filtered through a 0.2 μm cellulose acetate filter immediately (within 3 minutes) after collection and stabilized with ethanol (20% sample, 80% ethanol). UPLC (Acquity UPLC, Waters Corporation, Milford, MA) fitted with a UV photodiode array detector was used to quantify the amount of fenretinide in each sample. Two component gradient chromatography was performed using a 0.1% formic acid

solution in water as Component I and methanol as Component II. The flow rate was set at 0.4 mL/min with an initial isocratic condition of 40% Component I and 60% Component II for 0.5 minutes. Next, a linear gradient to 10% Component I was employed for 1.5 minutes after which the system was maintained at 10% Component I for an additional 2 minutes. Finally, the system was reconditioned at 40% Component I for 0.5 minutes prior to the next injection cycle. The column used in the analyses was a Kinetex C18 1.7 μm 50 × 2.1 mm (Phenomenex Inc., Torrance, CA) which was maintained at 30°C. Under these conditions the retention time for fenretinide was 2.5 minutes. Detection by UV spectrometry was obtained at 364 nm. The lower limit of quantification was 10 ng/mL, and the lower limit of detection was 5 ng/mL. All experiments were done in triplicate.

## Cell Culture

Caco-2 cells (passage 40-45) were grown at 37°C, 5% $CO_2$, and 90% relative humidity. Caco-2 cells were seeded onto 12-well, 3.0 μm pore size Transwell® inserts (Corning Incorporated, Corning, NY) at a density of $6.7\times10^4$cells/cm$^2$, and the culture medium was Dulbecco's Modified Eagle Medium (DMEM) with high glucose supplemented with 10% fetal bovine serum, 1% L-glutamine, 1% sodium pyruvate, 1% non-essential amino acids, and 1% antibiotics. The cells were allowed to differentiate for 23-25 days before experimentation. Transepithelial electrical resistance (TEER) of the monolayer was measured using an epithelial volt-ohmmeter (EVOM, WPI Inc., USA)to verify monolayer integrity. Lucifer yellow rejection assays confirmed that a TEER greater than 300 Ω·cm$^2$, corrected for background TEER contributed by the blank filter and culture medium, was sufficient to produce a Lucifer yellow permeability ($P_{app}$) of ≤ 5-12 nm/s.

## Caco-2 Permeability Studies

The transport medium contained 25 mM HEPES, 5 mM glucose, 145 mMNaCl, 3 mMKCl, 1 mM $CaCl_2$, 0.5 mM $MgCl_2{\cdot}6H_2O$, and 1 mM $NaH_2PO_4$ (pH 7.4) [30]. After 30 minutes incubation with the transport buffer, the donor compartment was loaded with approximately 50 μM of either unformulated fenretinide as a control or formulated fenretinide in transport buffer (concentration calculation based on drug loading and drug recovery), while transport buffer containing 4% bovine serum albumin (BSA) was loaded into the receiving compartment. BSA was utilized to maintain sink conditions in the receiving compartment and to saturate unspecific binding sitesand thus mimics the physiological presence of albumin within the capillary lumen [31]. Samples were taken from the receiver compartment at 30 minutes, 1 h, 2 h, 3 h, and 4 h, replacing the media in the receiver compartment with fresh transport buffer with 4% BSA. Throughout the experiment, the Transwell plates were incubated at 37°C and lightly shaken. TEER readings were taken throughout the experiment, and only those monolayers displaying TEER values greater than 300 Ω·cm$^2$ were used in studies. All experiments were done in triplicate.

## Fenretinide Extraction Following Caco-2 Permeability Studies

At the conclusion of the 4 hour study, the contents of the donor compartment and receiver compartment were completely removed. Samples from the donor compartment and receiver compartment were incubated with ethanol (20% sample, 80% ethanol) overnight to

precipitate the BSA and to solubilize all fenretinide in the sample. The receiver compartment was incubated with 2.0 mL ethanol overnight. The cells were rinsed with 0.5 mL ice-cold HBSS, and the cells were scraped from the filter. A final rinse with 0.5 mL ice-cold HBSS was done to ensure that all cells were collected. The cells were subjected to a freeze-thaw cycle and centrifuged at 13,000 RPM for 10 minutes. The supernatant was removed (representing the drug content in the cell cytosol), stabilized with ethanol (20% sample, 80% ethanol), and allowed to incubate overnight. The pellet remaining in the centrifuge tube (representing the drug content in the cell membrane) was also incubated with 1.5 mLethanol overnight [32]. The filter, now devoid of cells, was additionally incubated overnight with 2.0 mL of ethanol. On the following day, all samples were then centrifuged at 13,000 RPM for 10 minutes, and the supernatant solutions were analyzed for fenretinide. Fenretinide quantification was done by the same UPLC-UV procedure employed for the releasestudies. Mass balance was calculated for all experiments to ensure complete accounting of fenretinide within the system. Traditional apparent permeability coefficient calculations assume linear drug transport, negligible back flux, and no mass balance issues such as cellular retention or drug binding to test apparatus [33]. Therefore, to account for the drug bound to the apparatus, normalized flux was calculated which accounts for the whole permeated substance at the conclusion of the experiment. The normalized flux ($J$)for each formulation was calculated as the total amount of drug transported (including basolateral chamber and filter wash) (μg) divided by total experimental time (s), the membrane growth area ($cm^2$), and the initial drug concentration in the donor compartment at $t$=0.

### Statistical Analysis

Statistical comparisons were conducted between samples using ANOVA and the Holm-Sidak method for multiple pair-wise comparisons. Differences between two related parameters were considered statistically significant at $p < 0.05$. SigmaPlot (Systat Software, Inc., San Jose, CA) software was used for all statistical analysis.

## Results and Discussion

All of the formulations resulted in drypowder products. While the drug recovery may appear better for formulations A1, B1, and C1 at 111.12% ± 9.85%, 110.44% ± 17.82%, and 97.73% ± 16.49%, respectively, drug recoveries from formulations A2, B2, and C2 (96.13% ± 7.88%, 89.62% ± 7.00%, and 89.48% ± 7.70%, respectively) were far more consistent between batches as evidenced in the relatively lowerstandard deviations of the measurements (Figure 1). The relatively large standard deviations observed could be attributed to the small size of the prepared batches, resulting in greater percent variability in measurement among batches. The only significant statistical difference in drug recovery observed was formulations A1 and B1 compared to formulations B2 and C2 ($p \leq 0.018$). However, no correlation between drug content or polymer content and encapsulation efficiency was observed, and all formulations had greater than 89% encapsulation efficiency.

As the PVP content increased, the recovered particle size following lyophilization became more consistent with the pre-lyophilization particle size, especially for formulations A1, B1, and C1 (Figure 2). When the amount of lactose is increased (corresponding to formulations

A2, B2, and C2), the positive effects of increased polymer for the recovery of the post-lyophilized particle size are lessened. However, since a higher drug concentration in the formulations can be achieved with less lactose (A1, B1, and C1), a higher PVP content is preferable to a higher lactose content to stabilize the particle size because PVP contributes to the solubilization of the drug upon reconstitution. The average polydispersity index across all formulations was 0.202 ± 0.037 prior to lyophilization and was 0.223 ± 0.059 after lyophilization with no statistically significant change. Figure 3 compares the SEM micrographs of the physical mixture to the dry and reconstituted formulations. While the physical mixture had no consistent size or morphology, the lyophilized powder (Figure 3b) contained large plates or flakes of material with a distinct micro-structure upon higher magnification. When the formulations were reconstituted with water, uniform nanoparticles were observed, though with no distinct surface morphology (Figure 3c).

In the reversing DSC thermograms (Figure 4), fenretinide had one melting endotherm with onset of 173.57°C; lactose had two endotherms, one at peak onset of 136.52°C corresponding to the loss of water of crystallization [34] and another at 209.99°C corresponding to the melting of lactose. PVP had a broad endotherm starting at113.93°C corresponding to its dehydration. Fenretinide has been reported to be present in at least two different polymorphic forms with melting peaks of 173-175°C [35] and178-181°C [1]. The physical mixture of fenretinide with lactose and PVP showed the characteristic endotherms for lactose and fenretinide (peak onsets at 172.12°C, 139.40°C, and 209.46°C), indicating no interaction between them. On the other hand, for all formulations no melting endotherms for fenretinide were detected, indicating that fenretinide was present in an amorphous state in the formulations. XRPD of unprocessed fenretinide shows a crystalline compound with peaks at $2\theta$ of 5.9°, 12.0°, 14.3°, 15.0°, 18.4°, 19.0°, 20.0°, 22.0°, 25.3°, and 26.5° (Figure 5). The XRPD analysisof the formulations showed no distinct peaks corresponding to fenretinide, rather simply the broad peaks indicative of amorphous materials and similar to that of PVP. In the physical mixture, the fenretinide characteristic peaks, most noticeable at 14.3° and 15.0°, are retained, confirming the crystalline nature of the drug. The absence of the fenretinide characteristic peaks in the formulations confirms the amorphous nature of the drug in the formulations, supporting the results of the thermal analysis.

Since the goal of the project is to enhance the permeability of fenretinide through the gut, the determination of fenretinide releasefrom the formulations was based on the formation of drug components smaller than 200 nm which is the pore size of the filters used in the releasestudies. This was selected so as to be below the cut-off size of 300 nm reported as the upper limit of the optimal particle size for permeability into Caco-2 cell membranes [36,37]. Therefore, the drug detected could include dissolved drug (*i.e.* in the molecular state), suspended nano-sized particles of drug, and drug/polymer nanoparticles. The purpose of this release study is to evaluate the available drug (in the form of dissolved drug or small drug particles) among different formulations over time. For the releasestudies, the maximum concentration of fenretinide was achieved by formulations A1, B1, A2, and B2(Table 2). A fenretinide control consisting of the drug alone without any processing was also studied; however, even though the aqueous solubility of fenretinide is reported to be approximately 5 ng/mL [38],for the control the concentration of dissolved drug was below the detectable

limit for all time points. At 24 hours, only formulations A1 and B1 had a detectable amount of drug after filtration with 23.6 ± 1.6 and 20.0 ± 3.3 ng/mL, respectively. Most of the formulations reached their peak released drug concentrations at 15 minutes (Figure 6). Interestingly, both C1 and C2, the formulations corresponding to the least amount of PVP, reached their maximum concentrations later, 30 minutes into the study, in addition to having significantly different drug concentrations than the other formulations for the first 3 hours of the study ($p \leq 0.039$). The highest drug release among the formulations was for formulation B1at 249.2 ± 35.5 ng/mL. Based on the releasestudies, a high PVP content, at or above a 4:1 polymer-to-drug ratio, is necessary to get maximal drug release, with lactose content as a lesser contributing factor to drug release. The best formulation appears to be B1 with a 4:1 polymer-to-drug ratio and 6:5 lactose-to-formulation ratio, balancing the need to maximize both drug content and drug release. These results were in agreement with the results of the particle size analysis, namely, that higher PVP content is preferable to higher lactose content. The decrease in drug concentration over timecould be due to aggregation of the nanoparticles or to Ostwald ripening. Degradation of fenretinide is an unlikely contributor to the observed reduction in drug release due to the absence of any new peaks in the chromatograms.

When the permeability of the formulations was evaluated in a Caco-2 cell model, the mass balance across the entire study was above 84%, though the control did have more variability than the formulations due to fenretinide's poorwater solubility (Table 3). Poor reproducibility and high variability are common for poorly water soluble compounds in a Caco-2 model [39]. Poor recovery, often less than 40% recovery, can lead to underestimation of apparent permeability and poor predictive power for further *in vivo* studies [40,41]. While the use of BSA in the receiver compartment may have attributed to the high drug recovery achieved in this study, cellular digestion and solvent chamber washes were the most significant contributors to the high recoveries in this study. The 300 $\Omega \cdot cm^2$ threshold determined by Lucifer yellow rejection assay is in agreement with typical values found in the literature [42]. The TEER readings for the formulations did drop below 300 $\Omega \cdot cm^2$ in the beginning of the studies but stabilized above the threshold over time (Figure 7). This pattern is typical of Caco-2 assays and is usually attributed to the mechanical stress of media aspiration and the addition of the sample solutions at $t$=0 [43,44]. The difference in the mean normalized flux between each treatment group and the control were significantly different ($p \leq 0.011$), and the flux was 3-4 times higher than the control for each formulation (Table 3).

The difference in the mean drug concentration in the cell membrane was not statistically different among the formulations and control group, while the cell cytosol and basolateral chamber showed significantly different results between the formulations and the fenretinide control (Figure 8). The amount of drug within the cell membrane, ranging from 11.07% ± 1.34% for B2 to 16.91% ± 2.78% for B1, is in agreement with the findings of Kokate *et al.* who found 13-15% of the initial amount of fenretinide within the cell membrane [32]. While some studies report minimal loss due to the cell monolayer [40], our studies revealed a significant proportion of the drug associated with the cell monolayer both within the cells and associated with the lipid membrane.

While the amount found in the basolateral chamber for each formulation is significant in comparison to the fenretinide control, this amount includes the drug found in the chamber and on the filter, with most drug found within the filter wash. This result indicates that the rate-limiting steps in the passage of fenretinide from the apical chamber to the basolateral chamber are poor partitioning from the cell membrane to the basolateral chamberas well as accumulation on the filter itself. Rate-limitation by the drug partitioning out of the cell monolayer restricts the applicability of the predictive nature of the Caco-2 model [45]. Further studies must be done to determine if and how significantly the Transwell filter inhibits the partitioning of the drug into the basolateral chamber. As with the release study, the permeability data do not discriminate among different drug forms (dissolved drug, suspended nano-sized particles of drug, and drug/polymer nanoparticles).

## Conclusions

The PVP-based fenretinide nanoparticles showed consistent particle sizes around 200 nm, with no evidence of crystalline fenretinide within the formulations, fast releasewith as high as 40% release after 15 minutes,and statistically significant normalized flux in a Caco-2 model compared to fenretinide alone. Formulation B1, containing 4:1 polymer-to-drug ratio and 6:5 lactose-to-formulation ratio, seems to be the optimal choice for further evaluation as an oral delivery formulation for fenretinide. Future work would include additional cell testing to evaluate the formulations effectiveness against cancer cell lines and *in vivo* evaluation of the effectiveness of the developed nanoparticles.

## Acknowledgements

This publication was made possible by funding from the National Institute of Health (NIH) grant numbers 5SC3GM102050-03 and 2G12MD007595-06 and the Louisiana Cancer Research Consortium (LCRC). The contents are solely the responsibility of the authors and do not necessarily represent the official views of the NIH or the LCRC.

## References

1. Moon RC, Thompson HJ, Becci PJ, Grubbs CJ, Gander RJ, Newton DL, Smith JM, Phillips SL, Henderson WR, Mullen LT, Brown CC, Sporn MB. N-(4-Hydroxyphenyl)retinamide, a new retinoid for prevention of breast cancer in the rat. Cancer Res. 1979; 39(4):1339–46. PubMed PMID: 421218. [PubMed: 421218]
2. Holmes WF, Soprano DR, Soprano KJ. Synthetic retinoids as inducers of apoptosis in ovarian carcinoma cell lines. J Cell Physiol. 2004; 199(3):317–29. PubMed PMID: 15095280. [PubMed: 15095280]
3. Sun SY, Li W, Yue P, Lippman SM, Hong WK, Lotan R. Mediation of N-(4-hydoxyphenyl)retinamide-induced apoptosis in human cancer cells by different mechanisms. Cancer Res. 1999; 59(10):2493–8. PubMed PMID: 10344763. [PubMed: 10344763]
4. Decensi A, Robertson C, Guerrieri-Gonzaga A, Serrano D, Cazzaniga M, Mora S, Gulisano M, Johansson H, Galimberti V, Cassano E, Moroni SM, Formelli F, Lien EA, Pelosi G, Johnson KA, Bonanni B. Randomized double-blind 2 x 2 trial of low-dose tamoxifen and fenretinide for breast cancer prevention in high-risk premenopausal women. J ClinOncol. 2009; 27(23):3749–56. doi: 10.1200/JCO.2008.19.3797. PubMed PMID: 19597031.
5. Veronesi U, Mariani L, Decensi A, Formelli F, Camerini T, Miceli R, Di Mauro MG, Costa A, Marubini E, Sporn MB, De Palo G. Fifteen-year results of a randomized phase III trial of fenretinide to prevent second breast cancer. Ann Oncol. 2006; 17(7):1065–71. PubMed PMID: 16675486. [PubMed: 16675486]

6. Mata NL, Lichter JB, Vogel R, Han Y, Bui TV, Singerman LJ. Investigation of oral fenretinide for treatment of geographic atrophy in age-related macular degeneration. Retina. 2013; 33(3):498–507. doi: 10.1097/IAE.0b013e318265801d. PubMed PMID: 23023528. [PubMed: 23023528]
7. Rao RD, Cobleigh MA, Gray R, Graham ML 2nd, Norton L, Martino S, Budd GT, Ingle JN, Wood WC. Phase III double-blind, placebo-controlled, prospective randomized trial of adjuvant tamoxifen vs. tamoxifen and fenretinide in postmenopausal women with positive receptors (EB193): an intergroup trial coordinated by the Eastern Cooperative Oncology Group. Med Oncol. 2011; 28(Suppl 1):S39–47. doi: 10.1007/s12032-010-9682-1. PubMed PMID: 20878269. [PubMed: 20878269]
8. Moore MM, Stockler M, Lim R, Mok TS, Millward M, Boyer MJ. A phase II study of fenretinide in patients with hormone refractory prostate cancer: a trial of the Cancer Therapeutics Research Group. Cancer ChemotherPharmacol. 2010; 66(5):845–50. doi: 10.1007/s00280-009-1228-x. PubMed PMID: 20082080.
9. Vaishampayan U, Heilbrun LK, Parchment RE, Jain V, Zwiebel J, Boinpally RR, LoRusso P, Hussain M. Phase II trial of fenretinide in advanced renal carcinoma. Invest New Drugs. 2005; 23(2):179–85. PubMed PMID: 15744595. [PubMed: 15744595]
10. Colombo N, Formelli F, Cantù MG, Parma G, Gasco M, Argusti A, Santinelli A, Montironi R, Cavadini E, Baglietto L, Guerrieri-Gonzaga A, Viale G, Decensi A. A phase I-II preoperative biomarker trial of fenretinide in ascitic ovarian cancer. Cancer Epidemiol Biomarkers Prev. 2006; 15(10):1914–9. PubMed PMID: 17035399. [PubMed: 17035399]
11. William WN Jr, Lee JJ, Lippman SM, Martin JW, Chakravarti N, Tran HT, Sabichi AL, Kim ES, Feng L, Lotan R, Papadimitrakopoulou VA. High-dose fenretinide in oral leukoplakia. Cancer Prev Res (Phila). 2009; 2(1):22–6. doi: 10.1158/1940-6207.CAPR-08-0100. PubMed PMID: 19139014. [PubMed: 19139014]
12. Sabichi AL, Lerner SP, Atkinson EN, Grossman HB, Caraway NP, Dinney CP, Penson DF, Matin S, Kamat A, Pisters LL, Lin DW, Katz RL, Brenner DE, Hemstreet GP 3rd, Wargo M, Bleyer A, Sanders WH, Clifford JL, Parnes HL, Lippman SM. Phase III prevention trial of fenretinide in patients with resected non-muscle-invasive bladder cancer. Clin Cancer Res. 2008; 14(1):224–9. doi: 10.1158/1078-0432.CCR-07-0733. PubMed PMID: 18172274. [PubMed: 18172274]
13. Schneider BJ, Worden FP, Gadgeel SM, Parchment RE, Hodges CM, Zwiebel J, Dunn RL, Wozniak AJ, Kraut MJ, Kalemkerian GP. Phase II trial of fenretinide (NSC 374551) in patients with recurrent small cell lung cancer. Invest New Drugs. 2009; 27(6):571–8. doi: 10.1007/s10637-009-9228-6. PubMed PMID: 19225720. [PubMed: 19225720]
14. Villablanca JG, London WB, Naranjo A, McGrady P, Ames MM, Reid JM, McGovern RM, Buhrow SA, Jackson H, Stranzinger E, Kitchen BJ, Sondel PM, Parisi MT, Shulkin B, Yanik GA, Cohn SL, Reynolds CP. Phase II study of oral capsular 4-hydroxyphenylretinamide (4-HPR/fenretinide) in pediatric patients with refractory or recurrent neuroblastoma: a report from the Children's Oncology Group. Clin Cancer Res. 2011; 17(21):6858–66. doi: 10.1158/1078-0432.CCR-11-0995. PubMed PMID: 21908574. [PubMed: 21908574]
15. Reynolds CP. Detection and treatment of minimal residual disease in high-risk neuroblastoma. Pediatr Transplant. 2004; 8(Suppl 5):56–66. PubMed PMID: 15125707. [PubMed: 15125707]
16. Children's Oncology Group (CCG 09709). Villablanca JG, Krailo MD, Ames MM, Reid JM, Reaman GH, Reynolds CP. Phase I trial of oral fenretinide in children with high-risk solid tumors: a report from the Children's Oncology Group (CCG 09709). J ClinOncol. 2006; 24(21):3423–30. Erratum in: J ClinOncol. 2006;24(25):4223. Reynolds, Patrick C [corrected to Reynolds, C Patrick]. PubMed PMID: 16849757.
17. Maurer BJ, Kalous O, Yesair DW, Wu X, Janeba J, Maldonado V, Khankaldyyan V, Frgala T, Sun BC, McKee RT, Burgess SW, Shaw WA, Reynolds CP. Improved oral delivery of N-(4-hydroxyphenyl)retinamide with a novel LYM-X-SORB organized lipid complex. Clin Cancer Res. 2007; 13(10):3079–86. PubMed PMID: 17505011. [PubMed: 17505011]
18. Kummar S, Gutierrez ME, Maurer BJ, Reynolds CP, Kang M, Singh H, Crandon S, Murgo AJ, Doroshow JH. Phase I trial of fenretinidelym-x-sorb oral powder in adults with solid tumors and lymphomas. Anticancer Res. 2011; 31(3):961–6. PubMed PMID: 21498721. [PubMed: 21498721]

19. Patel RP, Patel MM. Physicochemical characterization and dissolution study of solid dispersions of Lovastatin with polyethylene glycol 4000 and polyvinylpyrrolidone K30. Pharm Dev Technol. 2007; 12(1):21–33. PubMed PMID: 17484141. [PubMed: 17484141]
20. Six K, Verreck G, Peeters J, Brewster M, Van Den Mooter G. Increased physical stability and improved dissolution properties of itraconazole, a class II drug, by solid dispersions that combine fast- and slow-dissolving polymers. J Pharm Sci. 2004; 93(1):124–31. PubMed PMID: 14648642. [PubMed: 14648642]
21. Tran TT, Tran PH, Lee BJ. Dissolution-modulating mechanism of alkalizers and polymers in a nanoemulsifying solid dispersion containing ionizable and poorly water-soluble drug. Eur J Pharm Biopharm. 2009; 72(1):83–90. doi: 10.1016/j.ejpb.2008.12.009. PubMed PMID: 19141319. [PubMed: 19141319]
22. Jinno J, Kamada N, Miyake M, Yamada K, Mukai T, Odomi M, Toguchi H, Liversidge GG, Higaki K, Kimura T. Effect of particle size reduction on dissolution and oral absorption of a poorly water-soluble drug, cilostazol, in beagle dogs. J Control Release. 2006; 111(1-2):56–64. PubMed PMID: 16410029. [PubMed: 16410029]
23. Hancock BC, Zografi G. Characteristics and significance of the amorphous state in pharmaceutical systems. J Pharm Sci. 1997; 86(1):1–12. PubMed PMID: 9002452. [PubMed: 9002452]
24. Yu L. Amorphous pharmaceutical solids: preparation, characterization and stabilization. Adv Drug Deliv Rev. 2001; 48(1):27–42. PubMed PMID: 11325475. [PubMed: 11325475]
25. Mukharya A, Chaudhary S, Mansuri N, Misra AK. Solid-state characterization of lacidipine/PVP K(29/32) solid dispersion primed by solvent co-evaporation. Int J Pharm Investig. 2012; 2(2):90–6. doi: 10.4103/2230-973X.100048. PubMed PMID: 23119238.
26. Niemczyk AI, Williams AC, Rawlinson-Malone CF, Hayes W, Greenland BW, Chappell D, Khutoryanskaya O, Timmins P. Novel polyvinylpyrrolidones to improve delivery of poorly water-soluble drugs: from design to synthesis and evaluation. Mol Pharm. 2012; 9(8):2237–47. doi: 10.1021/mp300079x. PubMed PMID: 22738427. [PubMed: 22738427]
27. Papadimitriou S, Bikiaris D. Dissolution rate enhancement of the poorly water-soluble drug Tibolone using PVP, SiO2, and their nanocomposites as appropriate drug carriers. Drug Dev Ind Pharm. 2009; 35(9):1128–38. doi: 10.1080/03639040902787653. PubMed PMID: 19555245. [PubMed: 19555245]
28. Patel GV, Patel VB, Pathak A, Rajput SJ. Nanosuspension of efavirenz for improved oral bioavailability: formulation optimization, in vitro, in situ and in vivo evaluation. Drug Dev Ind Pharm. 2014; 40(1):80–91. doi: 10.3109/03639045.2012.746362. PubMed PMID: 23323843. [PubMed: 23323843]
29. Van den Mooter G, Wuyts M, Blaton N, Busson R, Grobet P, Augustijns P, Kinget R. Physical stabilisation of amorphous ketoconazole in solid dispersions with polyvinylpyrrolidone K25. Eur J Pharm Sci. 2001; 12(3):261–9. PubMed PMID: 11113645. [PubMed: 11113645]
30. Dahan A, Sabit H, Amidon GL. Multiple efflux pumps are involved in the transepithelial transport of colchicine: combined effect of p-glycoprotein and multidrug resistance-associated protein 2 leads to decreased intestinal absorption throughout the entire small intestine. Drug MetabDispos. 2009; 37(10):2028–36. doi: 10.1124/dmd.109.028282. PubMed PMID: 19589874.
31. Yamashita S, Furubayashi T, Kataoka M, Sakane T, Sezaki H, Tokuda H. Optimized conditions for prediction of intestinal drug permeability using Caco-2 cells. Eur J Pharm Sci. May; 2000 10(3): 195–204. PubMed PMID: 10767597. [PubMed: 10767597]
32. Kokate A, Li X, Jasti B. Transport of a novel anti-cancer agent, fenretinide across Caco-2 monolayers. Invest New Drugs. 2007; 25(3):197–203. PubMed PMID: 17146731. [PubMed: 17146731]
33. Tran TT, Mittal A, Gales T, Maleeff B, Aldinger T, Polli JW, Ayrton A, Ellens H, Bentz J. Exact kinetic analysis of passive transport across a polarizedconfluent MDCK cell monolayer modeled as a single barrier. J Pharm Sci. 2004; 93(8):2108–23. PubMed PMID: 15236458. [PubMed: 15236458]
34. Gombás A, Antal I, Szabó-Révész P, Marton S, Erõs I. Quantitativedetermination of crystallinity of alpha-lactose monohydrate by Near InfraredSpectroscopy (NIRS). Int J Pharm. 2003; 256(1-2): 25–32. PubMed PMID:12695008. [PubMed: 12695008]

35. Shealy YF, Frye JL, O'Dell CA, Thorpe MC, Kirk MC, Coburn WC Jr, Sporn MB. Synthesis and properties of some 13-cis- and all-trans-retinamides. J Pharm Sci. 1984; 73(6):745–51. PubMed PMID: 6737257. [PubMed: 6737257]

36. Andar AU, Hood RR, Vreeland WN, Devoe DL, Swaan PW. Microfluidic preparation of liposomes to determine particle size influence on cellular uptake mechanisms. Pharm Res. Feb; 2014 31(2):401–13. doi: 10.1007/s11095-013-1171-8. PubMed PMID: 24092051. [PubMed: 24092051]

37. Xu A, Yao M, Xu G, Ying J, Ma W, Li B, Jin Y. A physical model for thesize-dependent cellular uptake of nanoparticles modified with cationicsurfactants. Int J Nanomedicine. 2012; 7:3547–54. doi: 10.2147/IJN.S32188. PubMed PMID: 22848178. [PubMed: 22848178]

38. Li CY, Zimmerman CL, Wiedmann TS. Solubilization of retinoids by bile salt/phospholipid aggregates. Pharm Res. 1996; 13(6):907–13. PubMed PMID: 8792431. [PubMed: 8792431]

39. Liu H, Sabus C, Carter GT, Du C, Avdeef A, Tischler M. In vitro permeabilityof poorly aqueous soluble compounds using different solubilizers in the PAMPAassay with liquid chromatography/ mass spectrometry detection. Pharm Res. 2003; 20(11):1820–6. PubMed PMID: 14661927. [PubMed: 14661927]

40. Cai X, Walker A, Cheng C, Paiva A, Li Y, Kolb J, Herbst J, Shou W, Weller H. Approach to improve compound recovery in a high-throughput Caco-2 permeabilityassay supported by liquid chromatography-tandem mass spectrometry. J Pharm Sci. 2012; 101(8):2755–62. doi: 10.1002/jps. 23194. PubMed PMID:22611052. [PubMed: 22611052]

41. Krishna G, Chen K, Lin C, Nomeir AA. Permeability of lipophilic compounds indrug discovery using in-vitro human absorption model, Caco-2. Int J Pharm. 2001; 222(1):77–89. PubMed PMID: 11404034. [PubMed: 11404034]

42. van Breemen RB, Li Y. Caco-2 cell permeability assays to measure drugabsorption. Expert Opin Drug MetabToxicol. 2005; 1(2):175–85. PubMed PMID: 16922635.

43. Fischer SM, Brandl M, Fricker G. Effect of the non-ionic surfactant Poloxamer 188 on passive permeability of poorly soluble drugs across Caco-2 cellmonolayers. Eur J Pharm Biopharm. 2011; 79(2):416–22. doi:10.1016/j.ejpb.2011.04.010. PubMed PMID: 21549839. [PubMed: 21549839]

44. Frank KJ, Westedt U, Rosenblatt KM, Hölig P, Rosenberg J, Mägerlein M, Brandl M, Fricker G. Impact of FaSSIF on the solubility and dissolution-/permeation rateof a poorly water-soluble compound. Eur J Pharm Sci. 2012; 47(1):16–20. doi: 10.1016/j.ejps.2012.04.015. PubMed PMID: 22579958. [PubMed: 22579958]

45. Buckley ST, Fischer SM, Fricker G, Brandl M. In vitro models to evaluate thepermeability of poorly soluble drug entities: challenges and perspectives. Eur J Pharm Sci. 2012; 45(3):235–50. doi: 10.1016/j.ejps.2011.12.007. PubMed PMID: 22178532. [PubMed: 22178532]

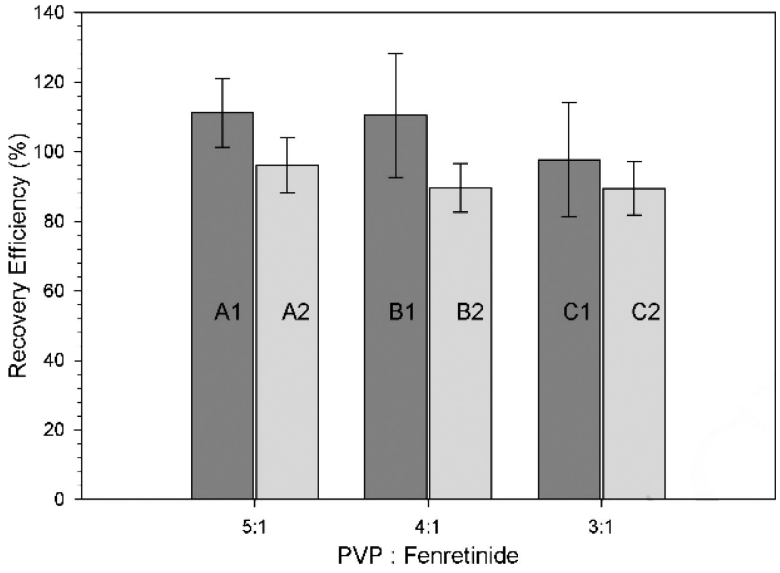


**Figure 1.**
Drug recovery efficiency following formulation as a PVP solid dispersion.

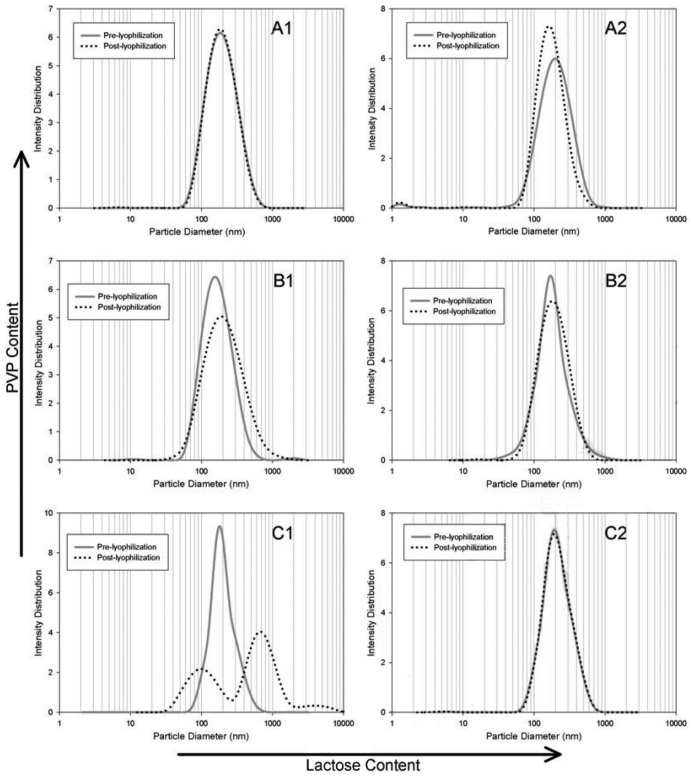


**Figure 2.**
Particle size distribution before and after lyophilization.

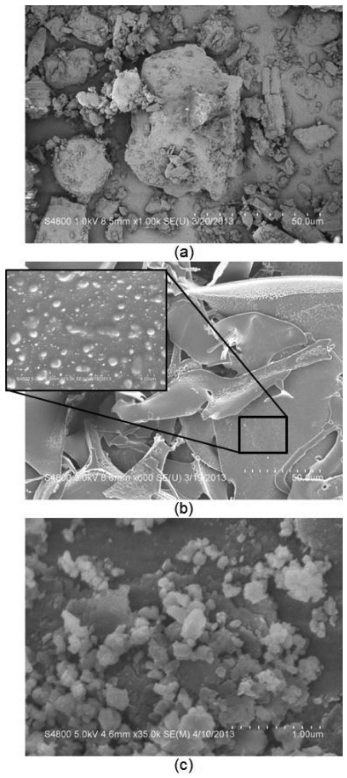


**Figure 3.**
Representative SEM micrographs of the (a) physical mixture, (b) post-lyophilization powdered sample, and (c) post-lyophilization sample reconstituted in water.

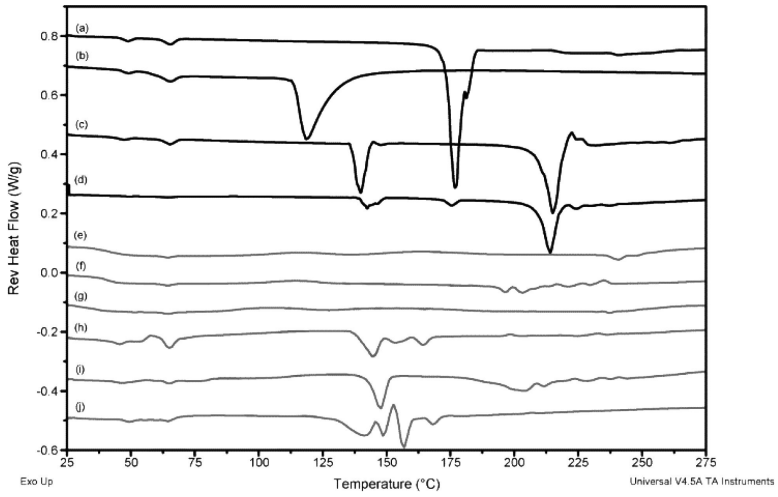


**Figure 4.**

mDSC scans (exo up) of reversing heat flow for (a) fenretinide, (b) PVP, (c) lactose, (d) physical mixture, (e) A1, (f) B1, (g) C1, (h) A2, (i) B2, and (j) C2.

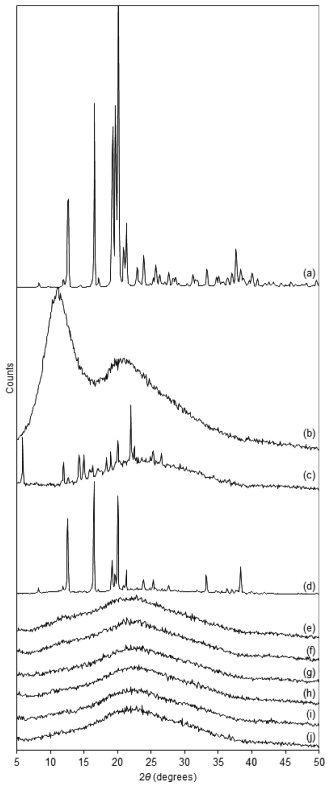


**Figure 5.**

XRPD patterns for (a) lactose, (b) PVP, (c) fenretinide, (d) physical mixture, (e) A1, (f) B1, (g) C1, (h) A2, (i) B2, and (j) C2.

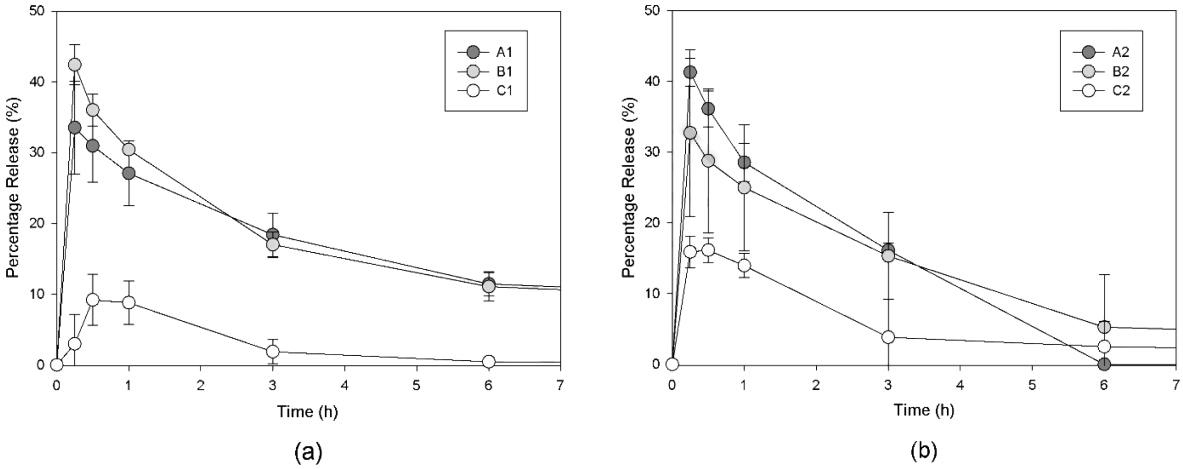


**Figure 6.**

Releaseprofiles in SIF for formulations (a) A1, B1, and C1 and (b) A2, B2, and C2. Data represent mean ± standard deviation.

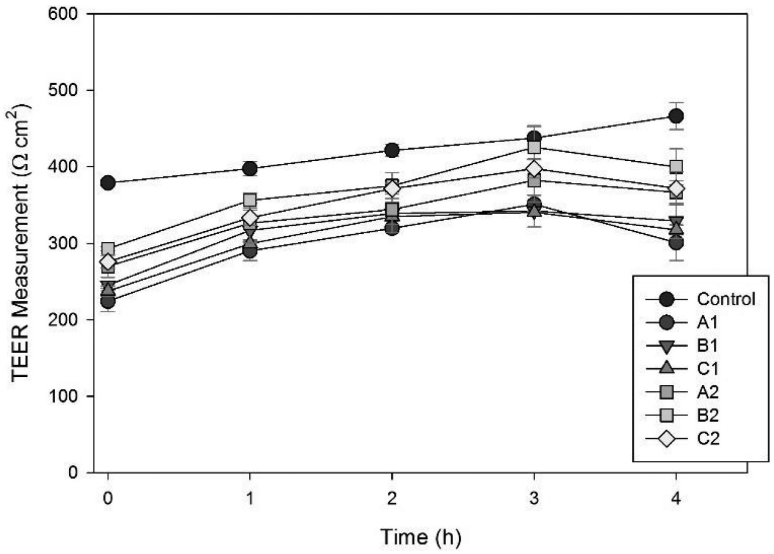


**Figure 7.**

TEER measurements, subtracting the TEER reading of a blank control filter, for the Caco-2 monolayers for each formulation. Data represent mean ± standard deviations.

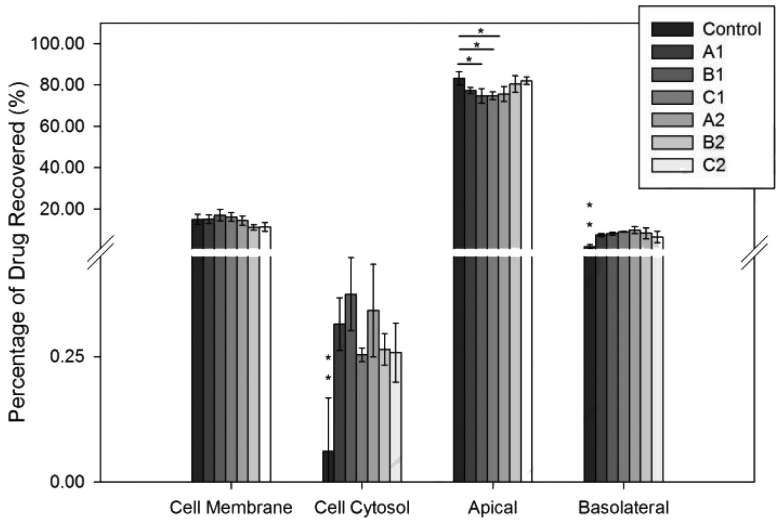


**Figure 8.**

Amount of drug recovered (as a percentage of the amount of drug loaded into the donor compartment) following 4 hours incubation with Caco-2 cells. The drug concentrations in both the basolateral compartment and in the cell cytosol for the formulation groups were all statistically different from the control (** $p \leq 0.02$). In the apical compartment, formulations B1, C1, and A2 had significantly different drug concentrations than the control (* $p \leq 0.037$).

**Table 1**

Formulation Compositions

| Formulation | PVP (mg) | Fenretinide (mg) | Lactose (mg) | PVP:Fenretinide | | Theoretical Drug Concentration (% w/w) |
|---|---|---|---|---|---|---|
| A1 | 20.83 | 4.17 | 30.0 | 5 | 1 | 7.58% |
| B1 | 20.00 | 5.00 | 30.0 | 4 | 1 | 9.09% |
| C1 | 18.75 | 6.25 | 30.0 | 3 | 1 | 11.36% |
| A2 | 20.83 | 4.17 | 60.0 | 5 | 1 | 4.90% |
| B2 | 20.00 | 5.00 | 60.0 | 4 | 1 | 5.88% |
| C2 | 18.75 | 6.25 | 60.0 | 3 | 1 | 7.35% |

## Table 2

Summary of ReleaseStudy Data

| Sample | $A_{max}$ [a] (%, mean ± SD) | $T_{max}$ [b] (minutes) | $C_{max}$ [c] (ng/mL, mean ± SD) | $C_6$ [d] (ng/mL, mean ± SD) |
|---|---|---|---|---|
| A1 | 33.5 ± 6.6 | 15 | 198.7 ± 29.1 | 68.1 ± 7.6 |
| B1 | 42.4 ± 2.8 | 15 | 249.2 ± 35.5 | 65.6 ± 17.3 |
| C1 | 9.2 ± 3.6 | 30 | 52.9 ± 19.7 | 2.4 ± 3.4 |
| A2 | 41.3 ± 2.0 | 15 | 137.5 ± 2.0 | BDL |
| B2 | 32.7 ± 11.8 | 15 | 112.4 ± 41.5 | 18.2 ± 25.8 |
| C2 | 16.1 ± 1.7 | 30 | 67.2 ± 7.3 | 10.6 ± 14.9 |

BDL = below detectable limit

[a] maximum amount (μg) measured in solution as a percentage of the initial amount of drug (μg)

[b] time period at which maximum amount measured

[c] maximum concentration (ng/mL) measured in solution

[d] concentration (ng/mL) measured at the 6 hour time period

**Table 3**

Caco-2 Permeability Assay Data

| Batch | Normalized Flux ($\times 10^{-7}$ cm/sec, mean ± SD) | Drug Recovery (%, mean ±SD) |
|---|---|---|
| A1 | 21.0 ± 1.9 | 92.2 ± 0.5 |
| B1 | 23.0 ± 2.4 | 92.6 ± 3.7 |
| C1 | 23.3 ± 2.0 | 84.6 ± 4.9 |
| A2 | 29.2 ± 5.2 | 96.8 ± 2.1 |
| B2 | 23.3 ± 7.0 | 91.8 ± 2.8 |
| C2 | 21.1 ± 8.5 | 106.4 ± 3.9 |
| control | 6.5 ± 2.6 | 123.2 ± 15.2 |